

## High temperature electrical conductivity in piezoelectric lithium niobate

Killian Lucas,<sup>1,2</sup> Sévan Bouchy,<sup>1,2</sup> Pierre Bélanger,<sup>1,2</sup> and Ricardo J. Zednik<sup>1,2</sup>

<sup>1</sup>*Piezoelectricity and Ultrasonics Technologies and Materials Laboratory at ÉTS (PULÉTS)*

<sup>2</sup>*Department of Mechanical Engineering, École de Technologie Supérieure (ÉTS), Université du Québec, Montréal, Canada*

(\*Electronic mail: [ricardo.zednik@etsmtl.ca](mailto:ricardo.zednik@etsmtl.ca))

(Dated: 26 April 2022)

Lithium niobate is a promising candidate for use in high temperature piezoelectric devices due to its high Curie temperature ( $\approx 1483$  K) and strong piezoelectric properties. However, the piezoelectric behavior has in practice been found to degrade at various temperatures as low as 573 K, with no satisfactory explanation available in the literature. We therefore studied the electrical conductivity of congruent lithium niobate single crystals in the temperature range of 293 K to 1273 K with an 500 mV excitation at frequencies between 20 Hz and 20 MHz. An analytical model that generalizes the universal dielectric relaxation law with the Arrhenius equation was found to describe the experimental temperature and frequency dependence, and helped discriminate between conduction mechanisms. Electronic conduction was found to dominate at low temperatures, leading to low overall electrical conductivity. However, at high temperatures the overall electrical conductivity increases significantly due to ionic conduction, primarily with lithium ions ( $\text{Li}^+$ ) as charge carriers. This increase in electrical conductivity can therefore cause an internal short in the lithium niobate crystal, thereby reducing observable piezoelectricity. Interestingly, the temperature above which ionic conductivity dominates depends greatly on the excitation frequency: at a sufficiently high frequency, lithium niobate does not exhibit appreciable ionic conductivity at high temperature, helping explain the conflicting observations reported in the literature. These findings enable an appropriate implementation of lithium niobate to realize previously elusive high temperature piezoelectric applications.

### I. INTRODUCTION

Piezoelectricity is the reversible behavior of certain materials to create an internal electric field when mechanically strained. Although engineers exploit this property in a myriad of daily room temperature applications, ranging from microphones to telescopes, there is an increasing need to operate at high temperatures, often approaching 1273 K. For example, the failure of critical high-temperature components in nuclear power plants, petroleum refineries, airplane jet turbines, or electrochemical fuel cells, can lead to disastrous consequences; such failures could be avoided if real-time structural health monitoring (SHM) using piezoelectric ultrasound devices were possible. Lead zirconium titanate (PZT or  $\text{Pb}[\text{Zr}_x\text{Ti}_{1-x}]\text{O}_3$ ) is one of the most commonly used piezoelectric materials due to its high piezoelectric coefficients, but it suffers from a low Curie temperature ( $\approx 638$  K)<sup>1,2</sup>: this temperature represents the theoretical limit, above which piezoelectricity is no longer possible. On the other hand, materials like gallium phosphate ( $\text{GaPO}_4$ ) have a high Curie temperature ( $\approx 1243$  K)<sup>2</sup>, but their piezoelectric coefficients are orders of magnitude lower than those of PZT crystals. Lithium niobate ( $\text{LiNbO}_3$ ) is a promising high temperature candidate, as it combines relatively high piezoelectric coefficients with a high piezoelectric Curie temperature ( $\approx 1483$  K)<sup>3</sup>, in contrast to most piezoelectric materials that may possess one but not the other. Although  $\text{LiNbO}_3$  has for years attracted considerable scientific and industrial interest due to its excellent electro-optic and acoustic properties<sup>4,5</sup>, this material's promising high temperature piezoelectric behavior is less commonly exploited by industry. Indeed, practical applications of lithium niobate have found that the experimentally observable piezoelectric behavior can degrade well be-

low the Curie temperature. The literature reports practical piezoelectric limits as low as 573 K, although there is significant variability<sup>6-12</sup>. In contrast, other researchers<sup>8,13-15</sup> have demonstrated that lithium niobate keeps its piezoelectric properties for several hours and even days in high temperature environments. This inconsistency and uncertainty is largely a result of the unknown mechanisms by which the piezoelectric properties of lithium niobate degrade. Why is piezoelectricity experimentally observable in some cases but not in others, even when well below the Curie temperature? Chemical or physical decomposition is often cited, but no satisfactory explanation has yet been accepted. For example, oxidation or lithium evaporation have been studied but shown to not be significant at ambient pressures<sup>9,16,17</sup>. Other authors have hypothesized that the degradation of piezoelectric behavior observed in some experiments may be due to the gradual apparition of electrical conductivity with increasing temperature; such electrical conductivity would short-circuit any internal piezoelectric polarization, but the conduction mechanisms are poorly understood<sup>16,18-21</sup>. The present study therefore endeavors to clarify this confusion reported in the literature by helping to understand possible electrical conduction mechanisms of lithium niobate that may cause piezoelectric degradation at high temperatures.

### II. EXPERIMENTAL METHODS

Congruent lithium niobate single crystals ( $10 \times 10 \times 0.495$  mm) with a Y-cut orientation in the thickness direction were grown by the Czochralski method. Symmetrical 100 nm thick platinum electrodes ( $10 \times 8.2$  mm) on 20 nm thick titanium adhesion layers were deposited onto both sides of the square

crystal using physical vapor deposition. Electrical contact to the electrodes was made using platinum wire to prevent asymmetrical chemical potential gradients. The sample was heated in a furnace at ambient atmosphere to 1273 K in 50 K steps at a rate of 5 K/min. At each step, the temperature was held for 30 minutes before taking electrical measurements using an E4990A Impedance Analyzer (Keysight Technologies).

### III. RESULTS AND DISCUSSION

#### A. Temperature dependence of conductivity

The electrical conductivity of lithium niobate was measured in 50 K intervals from room temperature to 1273 K with a 500 mV excitation over a frequency sweep between 20 Hz and 20 MHz. The measured conductivity as a function of temperature at three representative excitation frequencies is shown in Fig. 1. For clarity, only three representative frequencies are shown in Fig. 1, but the trends apply to all measured frequencies between 20 Hz and 20 MHz.

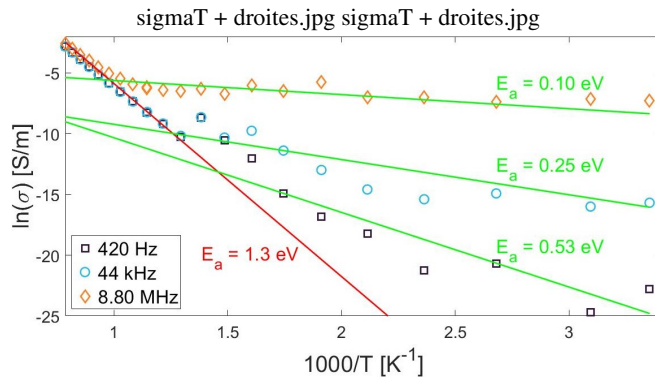


FIG. 1. Electrical conductivity of lithium niobate single crystal for representative 500 mV excitation frequencies. Straight lines represent activation energies from Eq. 1.

Lithium niobate is known to exhibit increased electrical conductivity at higher temperatures<sup>22</sup>, consistent with our observations. However, we find is that this conductivity depends on both temperature and excitation frequency. As shown in Fig. 1, high temperature behavior follows the red slope (for all frequencies) while low temperature behavior follows the green slope (for all frequencies). For any given frequency, the slopes are the same, with the only difference being the transition temperature at which the behavior changes. This implies that the electrical conductivity follows an Arrhenius law with two different mechanisms: one regime for high temperatures and one regime for low temperatures. Eq. 1 below expresses the conductivity,  $\sigma(T)$ , as an Arrhenius law function of temperature :

$$\sigma(T) = B e^{\frac{-E_a}{k_B T}} \quad (1)$$

where  $k_B$  is the Boltzmann constant,  $T$  is the absolute temperature,  $E_a$  is the activation energy, and  $B$  is a proportionality factor.

The presence of distinct activation energies implies the existence of different conduction mechanisms. By fitting Eq. 1 to the measured conductivity data, the activation energy  $E_a$  was found to be  $\approx 1.3$  eV at high temperatures, regardless of excitation frequency. This contrasts with the activation energy at low temperatures of  $0.1 \sim 0.5$  eV.

Table I summarizes the activation energies of selected charge carriers in lithium niobate, as found in the literature.

	$e^-$	$Li^+$	$Nb^{5+}$	$O^{2-}$
$E_a$ (eV)	0.27 <sup>23</sup> 0.84 <sup>20,26</sup>	1.37 <sup>7</sup> 1.25 <sup>20</sup> 1.16 <sup>27</sup>	2.75 <sup>24</sup>	3.7 <sup>25</sup> 3.45 <sup>9</sup>
Average (eV)	0.64	1.26	2.75	3.52

TABLE I. Activation energies reported in the literature for the mobility of various charge carrying species in lithium niobate

The measured activation energies are therefore most consistent with the motion of electrons ( $e^-$ ) at low temperatures and lithium ions ( $Li^+$ ) at high temperatures.

Fig. 1 also shows that the transition between the low temperature electronic regime and the high temperature ionic regime depends on the excitation frequency. Since electrons have a significantly smaller effective mass compared to lithium ions, we would expect electrons to be better able to follow a high frequency alternating electric field excitation. Therefore a higher excitation frequency should be correlated with a wider temperature range for which electronic conduction dominates. This is consistent with our experimental observations, where electrons are found to be the dominant charge carrier over a wide temperature range when the excitation frequency is high.

#### B. Excitation frequency dependence of conductivity

The effect of excitation frequency on the conductivity of lithium niobate is shown in Fig. 2. For clarity, only four representative temperatures are shown, but the trend is consistent for all measured temperatures between 293 K and 1273 K.

Analogous to the temperature dependence, two distinct regimes are apparent: a low frequency regime and a high frequency regime. The low frequency regime exhibits a conductivity that is largely frequency independent (i.e. DC conductivity), while the conductivity in the high frequency regime increases with excitation frequency. This frequency response of the conductivity  $\sigma(\omega)$  can be described by the Curie-von Schweidler universal dielectric relaxation law, as described by Jonscher<sup>28</sup> :

$$\sigma(\omega) = \sigma_{DC} + A\omega^n \quad (2)$$

where  $\sigma_{DC}$  is the DC conductivity,  $\omega (= 2\pi f)$  is the angular excitation frequency,  $f$  is the excitation frequency in Hz, and  $A$  and  $n$  are constants. This expression is suitable for describing both electronic and ionic conductivity phenomena,

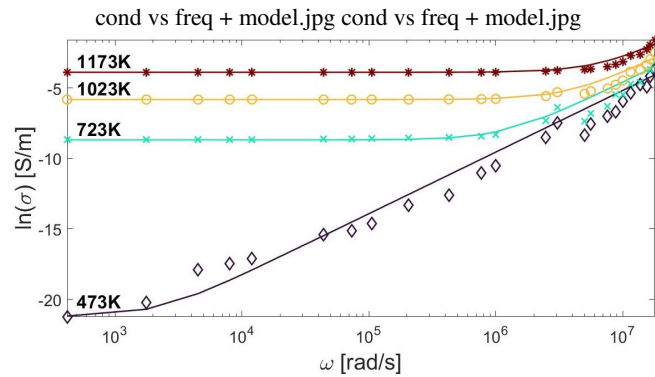


FIG. 2. Conductivity as a function of the excitation frequency for representative temperatures. Solid lines represent fit to Eq. 2

although possible frequency resonances are not taken into account and therefore omitted in our analysis. Using the experimentally measured conductivity, the coefficients  $A$  and  $n$  were determined for all temperature steps from 293 K to 1273 K using non-linear regression. The coefficient  $A$  was found to increase with temperature. According to Jonscher<sup>29</sup>, the coefficient  $n$  is not much affected by the temperature; this is consistent with our observation that  $n$  remains at a constant value of 1.9. The modeled conductivity, using eq. 2, is represented in fig. 2 by a solid line for each temperature. This model is in close agreement with the experimental observations.

### C. Modeling temperature and frequency dependence of conductivity

Having established that Eq. 1 adequately describes the temperature dependence of conductivity  $\sigma(T)$  and Eq. 2 adequately describes the excitation frequency dependence of conductivity  $\sigma(\omega)$ , it becomes natural to explore a combination of models. In particular, a generalized model for the conductivity  $\sigma(\omega, T)$  that includes both temperature and frequency effects is needed.

In principle, any of a number of charge carriers could contribute to the DC conductivity. If the concentration of charge carriers is low enough such that any interaction between them is negligible, the temperature dependence for each charge carrying species can be described by a relation of the form Eq. 1. As a result, the temperature dependence of the DC conductivity,  $\sigma_{DC}(T)$ , can be obtained by summing the contributions for each charge carrying species :

$$\sigma_{DC}(T) = \sum_{i=1}^4 B_i e^{-\frac{E_{a_i}}{k_B T}} \quad (3)$$

where the index  $i$  corresponds to one of the following charge carriers :  $E_{a_1}$  for electrons ( $e^-$ ),  $E_{a_2}$  for lithium ions ( $\text{Li}^+$ ),  $E_{a_3}$  for niobium ions ( $\text{Nb}^{5+}$ ), and  $E_{a_4}$  for oxygen ions ( $\text{O}^{2-}$ ).

However, the effect of the excitation frequency on the electrical conductivity may also vary with temperature, i.e.  $A(T)$ . Eq. 2 must therefore be generalized and combined with Eq. 3

to yield the temperature and frequency dependent conductivity,  $\sigma(\omega, T)$  :

$$\sigma(\omega, T) = \sum_{i=1}^4 B_i e^{-\frac{E_{a_i}}{k_B T}} + A(T)\omega^n \quad (4)$$

It is worth noting that we have limited our analysis to these four charge carrying species: electrons ( $e^-$ ), lithium ions ( $\text{Li}^+$ ), niobium ions ( $\text{Nb}^{5+}$ ), and oxygen ions ( $\text{O}^{2-}$ ). However, a wide range of other defects, including alternate oxidation states of these four species, impurities, etc. could have also been taken into consideration by expanding the summation index  $i$  used in Eq. 4. Nevertheless, we find that limiting our analysis to these four most important species is sufficient to adequately describe the experimental observations; other defects therefore only play a subordinate role in the electrical conductivity of our single crystal samples.

### D. Experimental frequency and temperature dependence of conductivity

The experimentally measured electrical conductivity is provided in Fig. 3 as a function of both temperature and excitation frequency.

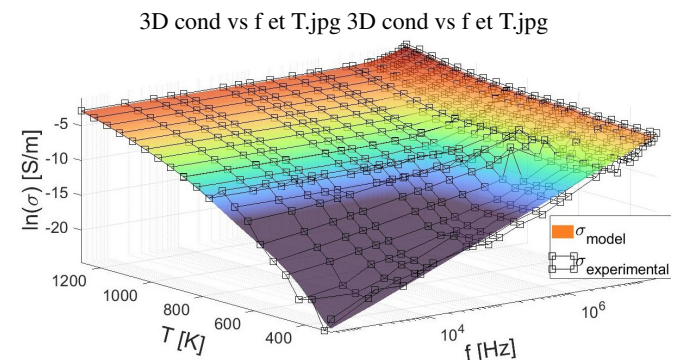


FIG. 3. Temperature and frequency dependence of electrical conductivity in lithium niobate

The model described by Eq. 4 was subsequently fit to the full experimental conductivity data by non-linear regression. As shown in Fig. 3, the model was found to closely follow the observed experimental conductivity across the entire temperature and frequency domain. The root mean square error (RMSE) of the model is around  $1.27 \times 10^{-3}$  and the R is 0.863 over the full temperature and frequency domain studied.

Table II summarizes the activation energies and pre-exponential factors  $B_i$  extracted from the entire experimental measurement data by fitting Eq. 4. These activation energies are consistent with the literature values listed in Table I and the activation energies found using the simpler model previously discussed in Section A and illustrated in Fig. 1.

	$e^-$	$Li^+$	$Nb^{5+}$	$O^{2-}$
$E_{a_i}$ (eV)	0.48	1.37	2.75	3.7
$B_i$ (S/m)	$2.46 \times 10^{-3}$	672	$1.35 \times 10^8$	$-4.13 \times 10^{11}$

TABLE II. Activation energies and coefficients  $B_i$  extracted by fitting Eq. 4 to the experimental data using non-linear regression.

### E. Electrical conduction mechanisms in lithium niobate

The model described by Eq. 4 is a linear sum of independent terms; it can therefore be used to deconvolute the relative contributions of each charge carrier to the overall conductivity. For example, Fig. 4 is a 2D cross-section through the 3D surface of Fig. 3 taken at a representative frequency of 12 kHz. The overall model (dashed line) fitting to the experimental data (x) is composed of the sum of four contributions (solid colored lines). Each contribution corresponds to one particular charge carrying species. Similar plots can be obtained for any desired frequency to identify the relative contribution of these four charge carriers at that frequency.

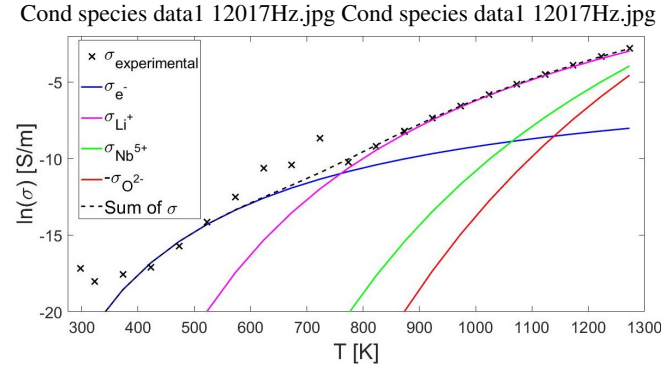


FIG. 4. Relative contribution of each charge carrier to the overall electrical conductivity at 12 kHz

For example, for an excitation frequency of 12 kHz at lower temperatures below 770 K, the electronic contribution is dominant and the overall conductivity is less than  $10^{-5}$  S/m. However, at temperatures above 770 K, the ionic charge carrier contributions begin to dominate (by multiple orders of magnitude) over the electronic contribution, and the overall conductivity rapidly increases. In particular, lithium ions ( $Li^+$ ) become the dominant charge carrier. This is consistent with the literature, in which several authors have found that lithium ions are the smallest and most mobile ions present in lithium niobate<sup>18,19,30</sup>. Ionic conduction in lithium niobate therefore occurs primarily by the charge carrier  $Li^+$  moving through the  $LiNbO_3$  lattice. This movement would be expected to be very sensitive to the concentration of lithium lattice site vacancies ( $V_{Li}'$ )<sup>17-19,27,31</sup>.

Niobium ions ( $Nb^{5+}$ ) may also potentially diffuse with the help of lithium vacancies, as the ionic radii of niobium ions ( $r_{Nb^{5+}} = 64 pm$ ) and lithium ions ( $r_{Li^+} = 76 pm$ ) are similar<sup>12,24</sup>. For the electronic conductivity, polarons and bipolarons may be involved<sup>23</sup>, which would also increase with

an increasing number of vacancies in the crystal. On the other hand, oxygen ions ( $O^{2-}$ ) are known to diffuse via interstitial sites rather than oxygen vacancies<sup>25</sup>, and would therefore be relatively unaffected by lithium vacancies.

Nevertheless, the contributions of niobium ions and oxygen ions only become significant at high temperatures above 1100 K. However, even at these high temperatures, their collective contribution to the electrical conductivity is overwhelmed by the dominance of lithium ions. This is consistent with Fig. 1, in which only two primary charge carriers are identifiable: electrons (at low temperatures) and lithium ions (at high temperatures).

The transition temperature  $T_{transition}$  above which the ionic conductivity (regardless of the ionic species) dominates over the electronic conductivity depends on the excitation frequency. As shown in Fig. 4, an excitation frequency of 12 kHz has a transition temperature of 770 K. Fig. 5 shows how  $T_{transition}$  varies over the excitation frequency domain studied.

As expected, the higher the excitation frequency, the higher the  $T_{transition}$  at which ionic conductivity becomes dominant. We find that  $T_{transition}$  remains  $\leq 800$  K for frequencies  $\leq 100$  kHz but then gradually increases to  $\geq 1200$  K for higher frequencies. With increasing temperature, the number of intrinsic defects, including vacancies, in the crystal grows and ions become more mobile. This increased mobility results in increasing ionic conductivity, dominated by lithium ion charge carriers.

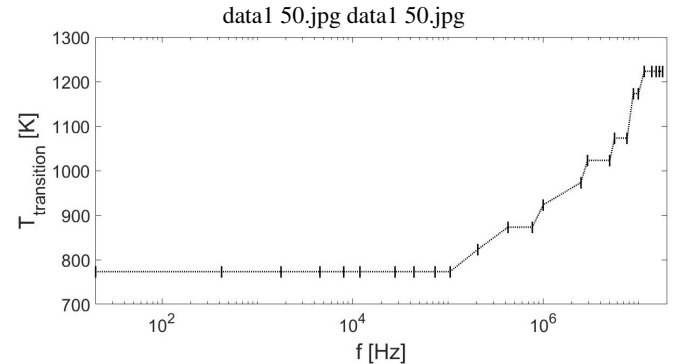


FIG. 5. Transition temperature  $T_{transition}$  at which the ionic conductivity dominates over the electronic conductivity as a function of excitation frequency.

Once the temperature and excitation frequencies are such that ionic conduction dominates, the overall conductivity begins to increase rapidly. This increasing conductivity would internally short a crystal, explaining why the piezoelectric behavior of lithium niobate may be experimentally unobservable under certain conditions for temperatures well below the Curie temperature.

Given this result, piezoelectric behavior would also be expected to be more readily observable at higher temperatures for stoichiometric lithium niobate (which is strictly  $LiNbO_3$ ) than for congruent lithium niobate (which is closer to  $Li_{0.485}Nb_{0.515}O_3$ ). Congruent lithium niobate is slightly lithium deficient (due to growing the crystal by the Czochralski method from a congruent melt); in other words, it has

a higher concentration of lithium lattice site vacancies and would therefore increase the mobility of lithium ion charge carriers, resulting in a lower  $T_{transition}$  for a given excitation frequency. Unfortunately authors are rarely explicit as to whether their measurements were conducted on congruent (more readily available, less expensive) or stoichiometric (less common, more expensive) lithium niobate single crystals.

This complex nature of the electrical conductivity in lithium niobate helps explain why the literature reports such contradictory results on the piezoelectric behavior. Whether or not piezoelectricity is practically observed in lithium niobate depends on temperature, excitation frequency, and composition. When the conditions are such that the electrical conductivity increases (due to predominantly lithium ion ( $Li^+$ ) conduction), internal shorting of the crystal can cancel out any piezoelectric polarization. This situation can occur below the theoretical Curie temperature, thereby suppressing the experimental observation of piezoelectricity.

## CONCLUSIONS

We report on the electrical conductivity in congruent lithium niobate from ambient temperature (293 K) to elevated temperature (1273 K) over a wide excitation frequency domain (20 Hz to 20 MHz). The analysis of the temperature response at different excitation frequencies revealed two different conductive processes that follow an Arrhenius relationship: electronic and ionic conductivity.

The transition temperature  $T_{transition}$  above which ionic conductivity dominates over electronic conductivity is excitation frequency dependent. By generalizing the universal dielectric relaxation law with the Arrhenius equation, an analytical model that simultaneously describes the dependence of electrical conductivity on both temperature and excitation frequency was developed. This strategy helped deconvolute the relative contributions of charge carrying species. This approach is consistent with the physics of an ionized gas and can therefore also be applied to a wide range of similar materials. For lithium niobate, the ionic conductivity that appears at higher temperatures was thereby confirmed to be dominated by lithium ion charge carriers ( $Li^+$ ) with an activation energy of 1.37 eV.

This improved understanding of electrical conductivity in lithium niobate helps explain the wide range of conflicting reports in the literature involving the degradation of piezoelectric behavior at temperatures significantly below the Curie temperature of 1483 K. This highlights the importance for researchers to explicitly state the measurement conditions and precise chemical composition of samples used in experiments.

The present results confirm the undeniable potential for lithium niobate as a high temperature piezoelectric material. From an applied physics standpoint, if a high temperature (> 573 K) application of piezoelectricity is envisioned, our results show the importance of selecting a stoichiometric composition and device design that uses as high an excitation frequency as is compatible with the implementation. In addition, methods that reduce the concentration or mobility of lithium

ions should also be explored. Although we limited our experimental studies to single crystal lithium niobate, we expect that polycrystalline samples should be more susceptible to high temperature degradation, as the increased ionic mobility along the grain boundaries would increase the susceptibility to an "internal short". A piezoelectric application envisioning high temperatures should therefore ideally employ a single crystal. These conditions will effectively prevent the appearance of significant electrical conductivity that could cause an internal short in the lithium niobate crystal, thereby degrading the piezoelectric behavior.

## AIP PUBLISHING DATA SHARING POLICY

The data that support the findings of this study are available from the corresponding author upon reasonable request.

## ACKNOWLEDGMENTS

The authors would like to thank Guillaume Boivin for technical assistance. The authors also wish to acknowledge the Natural Sciences and Engineering Research Council of Canada (NSERC) Discovery Grant RGPIN-2015-04185 and the École de Technologie Supérieure's Programme Impulsion for funding support.

## REFERENCES

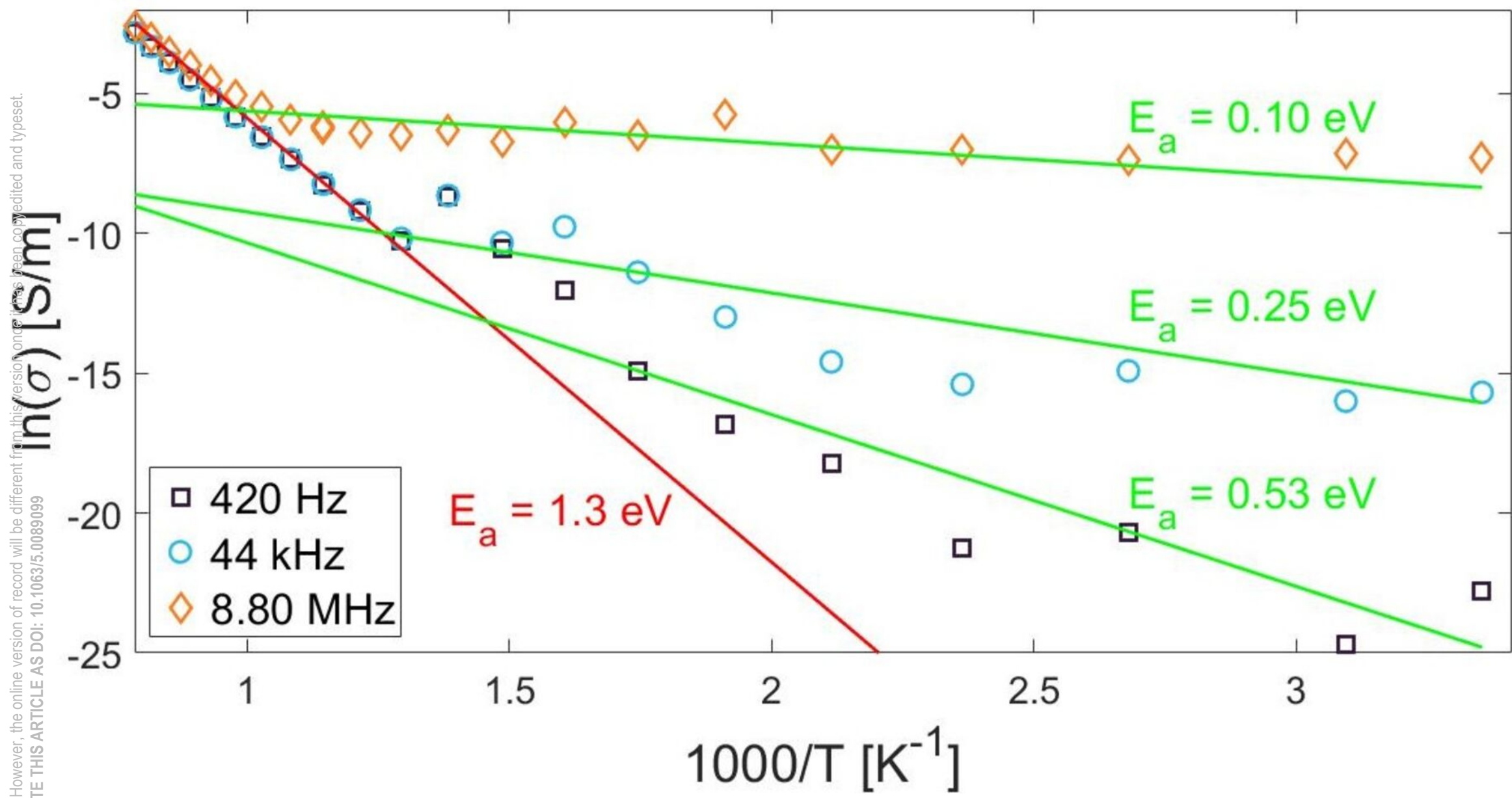
- W. R. C. B. Jaffe and H. L. Jaffe, *Piezoelectric Ceramics* (Academic Press, 1971).
- K. Shinekumar and S. Dutta, "High-temperature piezoelectrics with large piezoelectric coefficients," *J. Electron. Mater.* **44**, 613–622 (2015).
- J. R. Carruthers, G. E. Peterson, M. Grasso, and P. M. Bridenbaugh, "Non-stoichiometry and Crystal Growth of Lithium Niobate," *Journal of Applied Physics* **42**, 1846–1851 (1971).
- R. S. Weis and T. K. Gaylord, "Lithium niobate: Summary of physical properties and crystal structure," *Applied Physics A Solids and Surfaces* **37**, 191–203 (1985).
- R. T. Smith and F. S. Welsh, "Temperature Dependence of the Elastic, Piezoelectric, and Dielectric Constants of Lithium Tantalate and Lithium Niobate," *Journal of Applied Physics* **42**, 2219–2230 (1971).
- R. Fachberger, G. Bruckner, G. Knoll, R. Hauser, J. Biniash, and L. Reindl, "Applicability of  $LiNbO_3$ , langasite and  $GaPO_4$  in high temperature SAW sensors operating at radio frequencies," *IEEE Transactions on Ultrasonics, Ferroelectrics and Frequency Control* **51**, 1427–1431 (2004).
- A. Weidenfelder, J. Shi, P. Fielitz, G. Borchardt, K. Becker, and H. Fritze, "Electrical and electromechanical properties of stoichiometric lithium niobate at high-temperatures," *Solid State Ionics* **225**, 26–29 (2012).
- G. Ohlendorf, D. Richter, J. Sauerwald, and H. Fritze, "High-Temperature Electrical Conductivity and Electro-mechanical Properties of Stoichiometric Lithium Niobate," *Diffusion Fundamentals* **8** (2008).
- A. Weidenfelder, H. Fritze, P. Fielitz, G. Borchardt, J. Shi, K.-D. Becker, and S. Ganschow, "Transport and Electromechanical Properties of Stoichiometric Lithium Niobate at High Temperatures," *Zeitschrift für Physikalische Chemie* **226**, 421–429 (2012).
- A. Weidenfelder, M. Schulz, P. Fielitz, J. Shi, G. Borchardt, K.-D. Becker, and H. Fritze, "Electronic and Ionic Transport Mechanisms of Stoichiometric Lithium Niobate at High-Temperatures," *MRS Proceedings* **1519** (2013).

This is the author's peer reviewed, accepted manuscript. However, the online version of record will be different from this version once it has been copyedited and typeset.

PLEASE CITE THIS ARTICLE AS DOI: 10.1063/1.5008909

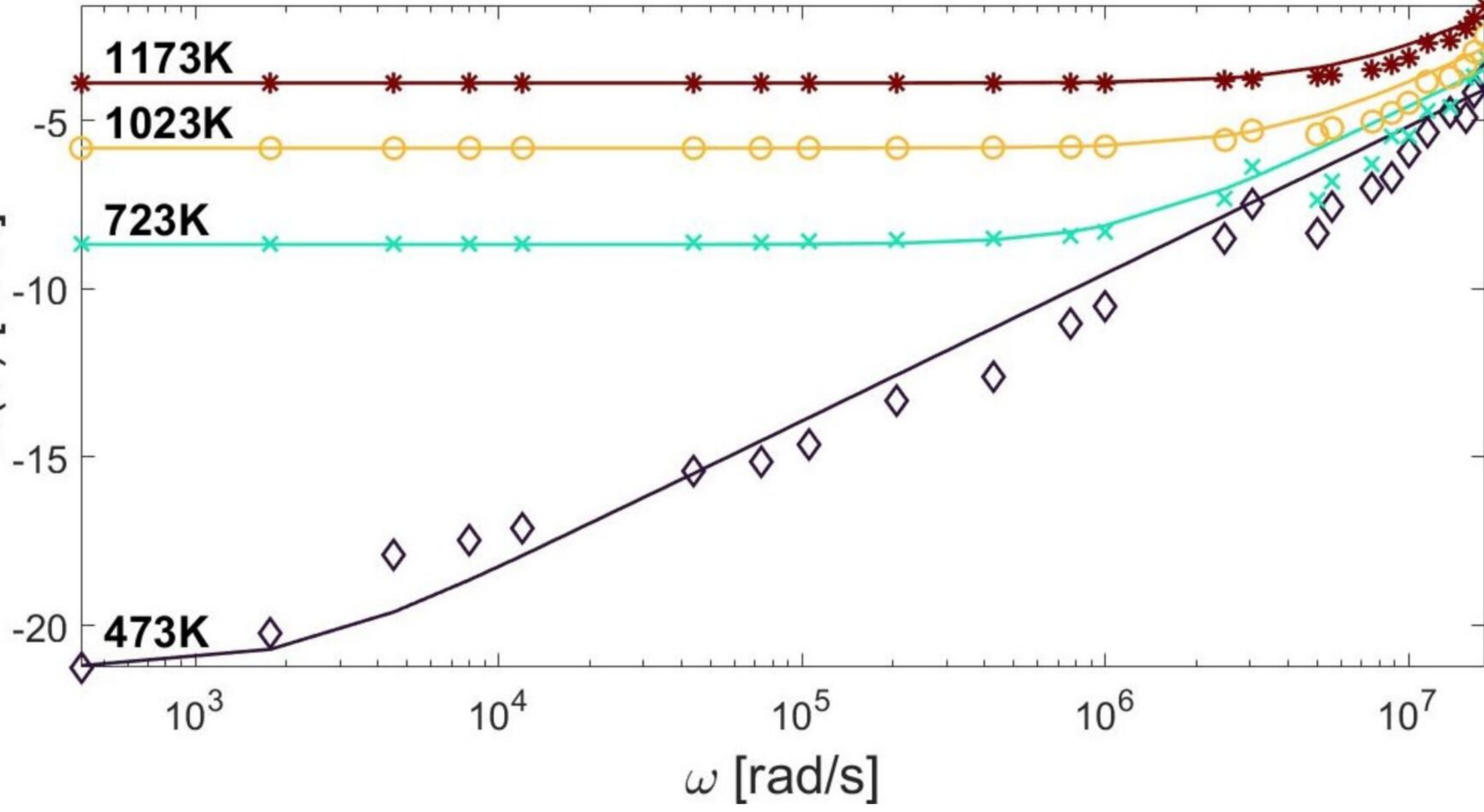
- <sup>11</sup>D. Damjanovic, "Materials for high temperature piezoelectric transducers," *Current Opinion in Solid State and Materials Science* **3**, 469–473 (1998).
- <sup>12</sup>E. Born, J. Hornsteiner, T. Metzger, and E. Riha, "Diffusion of Niobium in Congruent Lithium Niobate," *physica status solidi (a)* **177**, 393–400 (2000), publisher: John Wiley & Sons, Ltd.
- <sup>13</sup>A. Baba, C. T. Searfass, and B. R. Tittmann, "High temperature ultrasonic transducer up to 1000 C using lithium niobate single crystal," *Appl. Phys. Lett.* **97**, 4 (2010).
- <sup>14</sup>J. Hornsteiner, E. Born, G. Fischerauer, and E. Riha, "Surface acoustic wave sensors for high-temperature applications," in *Proceedings of the 1998 IEEE International Frequency Control Symposium (Cat. No.98CH36165)* (IEEE, Pasadena, CA, USA, 1998) pp. 615–620.
- <sup>15</sup>H. de Castilla, P. B elanger, and R. J. Zednik, "High temperature characterization of piezoelectric lithium niobate using electrochemical impedance spectroscopy resonance method," *Journal of Applied Physics* **122**, 244103 (2017).
- <sup>16</sup>A. S. Pritulenko, A. V. Yatsenko, and S. V. Yevdokimov, "Analysis of the nature of electrical conductivity in nominally undoped LiNbO<sub>3</sub> crystals," *Crystallography Reports* **60**, 267–272 (2015).
- <sup>17</sup>J. Shi, H. Fritze, G. Borchardt, and K.-D. Becker, "Defect chemistry, redox kinetics, and chemical diffusion of lithium deficient lithium niobate," *Physical Chemistry Chemical Physics* **13**, 6925 (2011).
- <sup>18</sup>B. Ruprecht, J. Rahn, H. Schmidt, and P. Heitjans, "Low-Temperature DC Conductivity of LiNbO<sub>3</sub> Single Crystals," *Zeitschrift f ur Physikalische Chemie* **226**, 431–437 (2012).
- <sup>19</sup>J. Rahn, E. H uger, L. D orrer, B. Ruprecht, P. Heitjans, and H. Schmidt, "Li self-diffusion in lithium niobate single crystals at low temperatures," *Physical Chemistry Chemical Physics* **14**, 2427 (2012).
- <sup>20</sup>A. El-Bachiri, F. Bennani, and M. Boussemamti, "Ionic and Polaronic Conductivity of Lithium Niobate," *Spectroscopy Letters* **47**, 374–380 (2014).
- <sup>21</sup>A. Mehta, E. K. Chang, and D. M. Smyth, "Ionic transport in LiNbO<sub>3</sub>," *Journal of Materials Research* **6**, 851–854 (1991).
- <sup>22</sup>M. N. Palatnikov, V. A. Sandler, N. V. Sidorov, and O. V. Makarova, "Investigation of the Piezoelectric Resonance in Stoichiometric LiNbO<sub>3</sub> Crystals at High Temperatures and Conductivities," *Physics of the Solid State* **61**, 1218–1222 (2019).
- <sup>23</sup>O. F. Schirmer, M. Imlau, C. Merschjann, and B. Schoke, "Electron small polarons and bipolarons in LiNbO<sub>3</sub>," *Journal of Physics: Condensed Matter* **21**, 123201 (2009).
- <sup>24</sup>P. Fielitz, G. Borchardt, S. Ganschow, R. Bertram, R. Jackson, H. Fritze, and K.-D. Becker, "Tantalum and niobium diffusion in single crystalline lithium niobate," *Solid State Ionics* **259**, 14–20 (2014).
- <sup>25</sup>P. Fielitz, O. Schneider, G. Borchardt, A. Weidenfelder, H. Fritze, J. Shi, K. Becker, S. Ganschow, and R. Bertram, "Oxygen-18 tracer diffusion in nearly stoichiometric single crystalline lithium niobate," *Solid State Ionics* **189**, 1–6 (2011).
- <sup>26</sup>A. El Bachiri, F. Bennani, and M. Boussemamti, "Dielectric and electrical properties of LiNbO<sub>3</sub> ceramics," *Journal of Asian Ceramic Societies* **4**, 46–54 (2016).
- <sup>27</sup>M. Masoud and P. Heitjans, "Impedance Spectroscopy Study of Li Ion Dynamics in Single Crystal, Microcrystalline, Nanocrystalline and Amorphous LiNbO<sub>3</sub>," *Defect and Diffusion Forum* **237-240**, 1016–1021 (2005).
- <sup>28</sup>A. K. Jonscher, *Universal relaxation law: a sequel to Dielectric relaxation in solids* (Chelsea Dielectrics Press, London, 1996).
- <sup>29</sup>A. K. Jonscher, "Dielectric relaxation in solids," *Journal of Physics D: Applied Physics* **32**, R57–R70 (1999).
- <sup>30</sup>Q. Wang, C. Liu, Y. Gao, Y. Ma, Y. Han, and C. Gao, "Mixed conduction and grain boundary effect in lithium niobate under high pressure," *Applied Physics Letters* **106**, 132902 (2015).
- <sup>31</sup>D. P. Birnie, "Analysis of diffusion in lithium niobate," *Journal of Materials Science* **28**, 302–315 (1993).

This is the author's peer reviewed, accepted manuscript. However, the online version of record will be different from this version once it has been copyedited and typeset.  
PLEASE CITE THIS ARTICLE AS DOI: 10.1063/5.0089099



This is the author's peer reviewed, accepted manuscript. However, the online version of record will be different from this version once it has been copyedited and typeset.  
PLEASE CITE THIS ARTICLE AS DOI: 10.1063/5.0089099

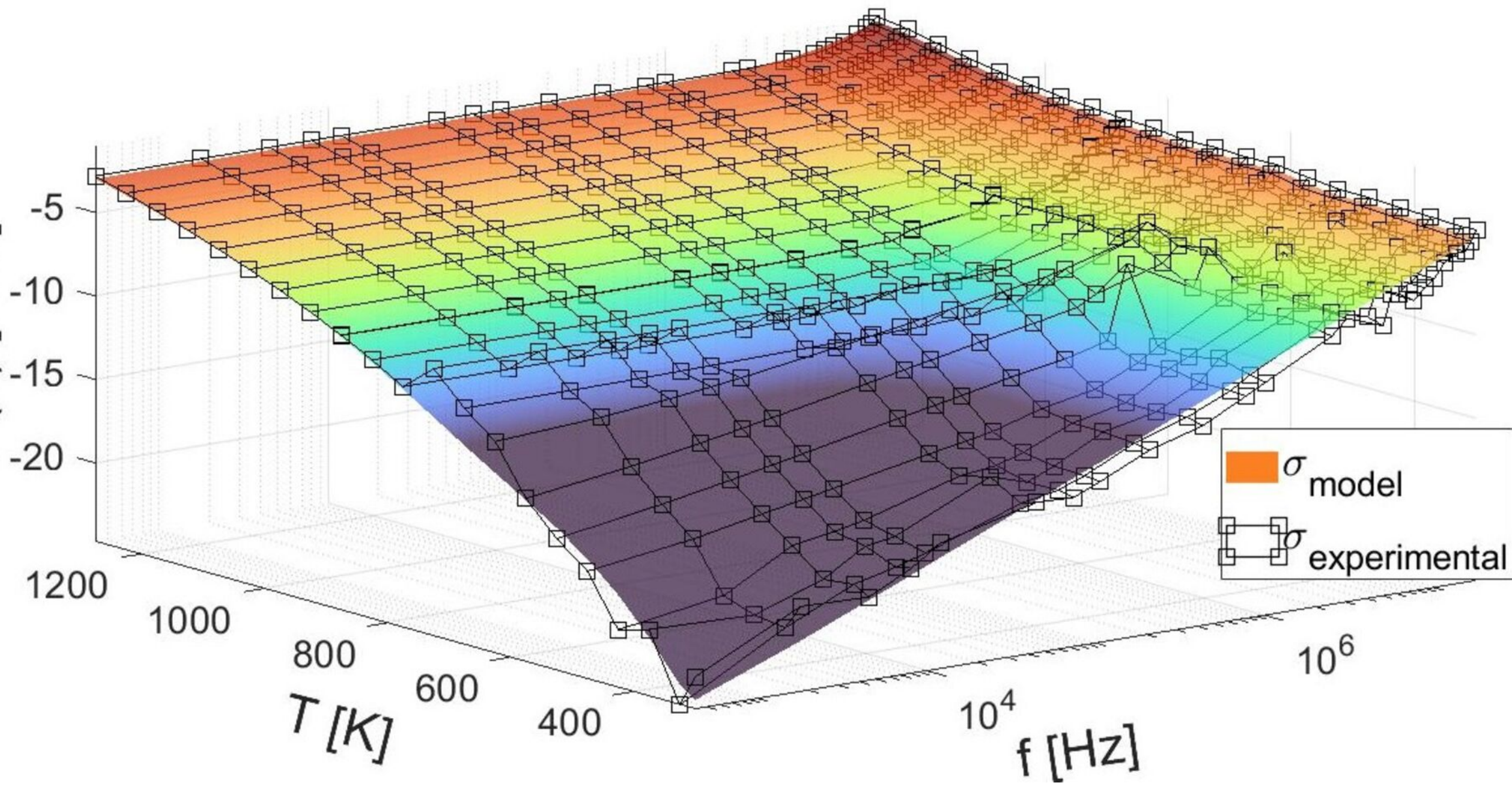
$\ln(\sigma)$  [S/m]



This is the author's peer reviewed, accepted manuscript. However, the online version of record will be different from this version once it has been copyedited and typeset.

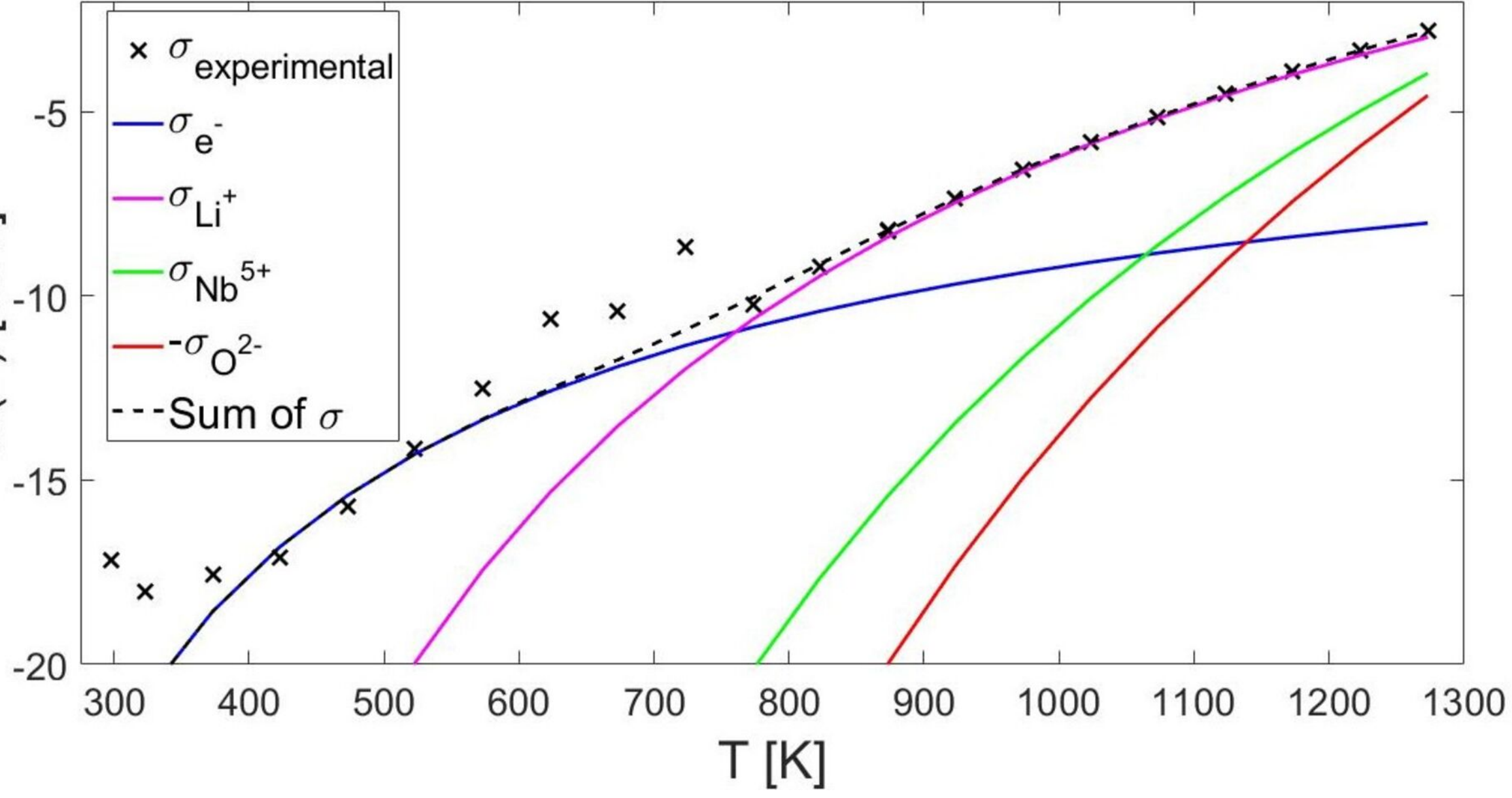
PLEASE CITE THIS ARTICLE AS DOI: 10.1063/5.0089099

$\ln(\sigma)$  [S/m]



This is the author's peer reviewed, accepted manuscript. However, the online version of record will be different from this version once it has been copyedited and typeset.  
PLEASE CITE THIS ARTICLE AS DOI: 10.1063/5.0089099

$\ln(\sigma)$  [S/m]



This is the author's peer reviewed, accepted manuscript. However, the online version of record will be different from this version once it has been copy edited and typeset.

PLEASE CITE THIS ARTICLE AS DOI: 10.1063/5.0089099

transition [K]

